Acta Cryst. (1999). B**55**, 517–524

Structure determination of lithium chloroacetate, lithium bromoacetate and lithium iodoacetate by powder diffraction

H. Ehrenberg,[a] B. Hasse,[b] K. Schwarz[b] and M. Epple[b]*

[a]*Darmstadt University of Technology, Materials Science, Petersenstrasse 23, D-64287 Darmstadt and Hamburg Synchrotron Radiation Laboratory (HASYLAB) at Deutsches Elektronen-Synchrotron (DESY), Notkestrasse 85, D-22603 Hamburg, Germany, and* [b]*Institute of Inorganic and Applied Chemistry, University of Hamburg, Martin-Luther-King-Platz 6, D-20146 Hamburg, Germany. E-mail: epple@xray.chemie.uni-hamburg.de*

(*Received 6 September 1998; accepted 3 March 1999*)

Abstract

Most halogenoacetates of alkali salts readily undergo a thermally induced polymerization reaction to poly(hydroxyacetic acid) in the solid state. The lithium salts represent a remarkable exception. The crystal structures of lithium chloroacetate, lithium bromoacetate and lithium iodoacetate were determined *ab initio* from synchrotron powder diffraction data. The three compounds are isostructural and differ considerably from the structures of sodium chloroacetate and silver chloroacetate, two compounds that undergo polymerization. Most likely, the strong polarizing effect of the small lithium cation is responsible for the unfavorable crystal structure in which each lithium cation is coordinated to four O atoms from four different halogenoacetate molecules. Lithium chloroacetate: a = 9.3882 (9), b = 4.8452 (4), c = 9.0119 (7) Å, β = 94.330 (5)°; lithium bromoacetate: a = 9.7165 (11), b = 4.8610 (6), c = 9.0228 (11) Å, β = 93.946 (5)°; lithium iodoacetate: a = 10.1812 (10), b = 4.8922 (8), c = 9.0468 (10) Å, β = 93.251 (5)°, all crystallizing in space group $P2_1/c$ with Z = 4.

1. Introduction

Within the context of our general studies of the reactivity of molecular crystals (Epple *et al.*, 1995; Epple & Seifert, 1996), we have studied the solid-state polymerization of halogenoacetates to polyglycolide (Epple & Tröger, 1996; Epple & Kirschnick, 1996; Epple & Herzberg, 1997), *e.g.*

$$Na^{+-}OOC-CH_2-Cl\ (s) \rightarrow NaCl\ (s) + 1/n[-OOC-CH_2]_n(s)$$

The polyester formed, polyglycolide or poly(hydroxyacetic acid), is well biodegradable to non-toxic products. Therefore, it is of considerable interest, *e.g.* in medical technology (Chiellini & Solaro, 1996). Washing out the salt formed with water leaves a highly porous polymer whose average pore size can be adjusted from *ca.* 300 nm to 1.5 µm. The reaction scheme can be transposed to most halogenoacetates of the general formula $M^{+-}OOC-CH_2-X$ (M = Li, Na, K, Rb, Cs, NH_4; X = Cl, Br, I; Epple & Herzberg, 1997). Interestingly, the major exceptions are the three lithium salts (chloroacetate, bromoacetate and iodoacetate) that do not undergo the above elimination reaction, but decompose or melt without polymerization (see Table 1).

By application of a multitude of analytical techniques, most of them applied *in situ*, we have demonstrated that probably neither liquid nor solid intermediates are involved in the elimination reaction (Epple *et al.*, 1996, 1997). Therefore, we may conclude that the reaction is determined by the crystal structure of the educts, *i.e.* occurs in a topochemical way, as found earlier for many other organic compounds (see *e.g.* Schmidt, 1971; Thomas, 1974; Wegner, 1977; Enkelmann, 1984; Boldyrev, 1990; Desiraju, 1995). It is of considerable interest to determine the crystal structures of the reaction educts, the halogenoacetates, in order to see whether the reactivity can be deduced from the arrangement of the molecules in the crystal, as demonstrated for other topochemical reactions.

Unfortunately, it is almost impossible to obtain suitable single crystals of halogenoacetates, as they all tend to crystallize in the form of thin and disordered platelets. The only case where we have been successful was silver chloroacetate $AgOOC-CH_2-Cl$, whose structure was determined by single-crystal X-ray diffraction (Epple & Kirschnick, 1997). Single crystal structures of ammonium fluoroacetate (Wei & Ward, 1976) and sodium fluoroacetate (Vedavathi & Vuayan, 1977) were reported in the literature. However, it is not known whether the fluoroacetates undergo polymerization upon heating (fluoroacetic acid and fluoroacetates are highly toxic compounds). The structure of ammonium chloroacetate was announced (Pepinsky *et al.*, 1957) but never published. Therefore, the structural basis for interpretation of the reactivity results is very limited.

Within the last few years it has become increasingly possible to solve crystal structures of organic molecules

Table 1. *Polymerizability of halogenoacetates as a function of halogen and metal (Epple & Herzberg, 1997)*

Ammonium chloroacetate oligomerizes in the melt, *i.e.* not in a solid-state reaction. '+': polymerization, '−': no polymerization.

	Cl	Br	I
Li	−	−	−
Na	+	+	−
K	+	+	+
Rb	+	+	+
Ag	+	+	Unstable
Cs	+	+	+
NH_4	(+)	Not studied	Not studied

ab initio from powder diffraction data (see *e.g.* Tremayne *et al.*, 1996; Kariuki *et al.*, 1996; Harris *et al.*, 1998; Dinnebier *et al.*, 1997*a*,*b* for some recent references), facilitated by the use of highly intense, collimated synchrotron radiation.

Recently, the structure of sodium chloroacetate $NaOOC-CH_2-Cl$ was determined *ab initio* by Monte Carlo methods from synchrotron powder data recorded at the Daresbury synchrotron (Elizabé *et al.*, 1997). Here we report on the determination of the structures of lithium chloro-, bromo- and iodoacetate from diffraction data recorded at the HASYLAB synchrotron source in Hamburg.

2. Experimental and data analysis

X-ray diffraction data were recorded at the powder diffractometer at beamline B2 at HASYLAB. The storage ring DORIS III was run with 4.444 GeV. The samples were studied at room temperature in rotating glass capillaries in Debye–Scherrer mode. Lithium chloroacetate and lithium bromoacetate were measured in 0.7 mm capillaries with a wavelength of 1.2841 Å (128.41 pm), and lithium iodoacetate was measured in a 1.0 mm capillary with 1.2006 Å (120.06 pm). The incoming beam was selected from the white beam with a Ge(111) double crystal monochromator. A custom-made vacuum chamber was used to avoid air scattering. Soller slits were placed between sample and detector. Data were collected from 5 to 60° 2θ (5 to 50° 2θ for lithium iodoacetate) in steps of 0.01° with an approximate counting time of 1–2 s at each point (scintillation counter). We chose the Soller setup due to the much higher diffraction intensity, although this gave a larger instrumental peak width. This is justified as lithium chloroacetate, bromoacetate and iodoacetate exhibit intrinsic peak widths (full width at half maximum) of 0.12, 0.12 and 0.10° 2θ at 7° 2θ and 0.34, 0.30 and 0.14° 2θ at 60° 2θ (50° 2θ for lithium iodoacetate), respectively. For lithium chloroacetate and bromoacetate this is definitely above the instrumental resolution, whereas for lithium iodoacetate it just meets the instrumental resolution for this low-resolution setup. We ascribe this intrinsic peak broadening to the limited crystallinity of the samples. The advantage of the synchrotron source was the tunability of the wavelength to reduce absorption effects and the much higher intensity of the incident beam. Higher resolution diffractometry was not necessary to solve and refine the structures.

For each sample several scans were recorded and summed to detect possible radiation damage. Only insignificant changes in the diffractograms were found in both cases, even after 10 or more hours of irradiation, indicating a sufficient stability of the compounds towards irradiation.

Lists of peak positions were extracted from the raw data by profile fitting and used as input for the indexing program *TREOR* (Werner *et al.*, 1985). For the three compounds similar monoclinic unit cells were suggested and the observed reflections were compatible with the extinction rules of space group $P2_1/c$. Based on this symmetry, profile matchings were performed using the program *FULLPROF* (Rodriguez-Carvajal, 1990) to both refine cell constants and profile parameters, and extract peak intensities. The obtained lists of reflections with corresponding intensities were used for the calculation of Patterson functions with *SHELXS*86 (Sheldrick, 1985). In the case of lithium bromoacetate, the derived Br-, O- and C-positions gave reasonable bonds and this structural model was used for Rietveld refinement with *FULLPROF* (Rodriguez-Carvajal, 1990). Li atoms were placed into suitable 'vacancies' and included in the refinement process. The effect of H atoms on the intensities is insignificant. Therefore, the H atoms could not be localized and have been omitted in the structure refinement.

The structure of lithium bromoacetate was solved first. Substitution of bromine by chlorine and iodine in the bromoacetate structure (including adjustment of the carbon–halogen distance) gave well refinable structure models for lithium chloroacetate and lithium iodoacetate, respectively.

The following parameters were refined with *FULLPROF* (Rodriguez-Carvajal, 1990): The scale factor S, 2 parameters for the preferred orientation ($G1$ and $G2$ in March's function), 4 cell parameters (a, b, c, β), zero-point shift, 2 profile parameters (η, X), 3 parameters for the peak width (u, v, w), 6 temperature factors for anisotropic refinement of the halogen (β_{11}–β_{23}), 1 common isotropic temperature factor for all non-halogen atoms (B_{iso}; for C, O, Li) and 18 coordinates for six independently refined atoms. For lithium bromoacetate, no preferred orientation was observed and consequently the parameters $G1$ and $G2$ were not refined. Altogether, this gave 38 refined parameters for lithium chloro- and iodoacetate and 36 parameters for lithium bromoacetate.

Correction for absorption was carried with *FULLPROF* (Rodriguez-Carvajal, 1990) by assuming an 80% packing of the sample in the capillary. All uncertainties

Table 2. *Experimental details*

	Lithium chloroacetate	Lithium bromoacetate	Lithium iodoacetate
Crystal data			
Chemical formula	$Li^+.C_2H_2ClO_2^-$	$Li^+.C_2H_2BrO_2^-$	$Li^+.C_2H_2IO_2^-$
Chemical formula weight	100.43	144.88	191.88
Cell setting	Monoclinic	Monoclinic	Monoclinic
Space group	$P2_1/c$	$P2_1/c$	$P2_1/c$
a (Å)	9.3882 (9)	9.7165 (11)	10.1812 (10)
b (Å)	4.8452 (4)	4.8610 (6)	4.8922 (8)
c (Å)	9.0119 (7)	9.0228 (11)	9.0468 (10)
β (°)	94.330 (5)	93.946 (5)	93.251 (5)
V (Å^3)	408.76 (6)	425.15 (9)	449.89 (10)
Z	4	4	4
Radiation type	Synchrotron	Synchrotron	Synchrotron
Wavelength (Å)	1.2841	1.2841	1.2006
Temperature (K)	298	298	298
Range used in refinement (2θ, °)	5–60	5–60	5–50
$G1$	1.51 (6)	1	0.53 (1)
$G2$	0.46 (6)	0	0.34 (5)
η	0.02 (4)	0.14 (6)	0.01 (2)
X	0.016 (2)	0.005 (3)	0.002 (2)
u	0.33 (6)	0.183 (1)	0.01 (2)
v	−0.01 (2)	0.02 (2)	0.017 (7)
w	0.015 (1)	0.014 (3)	0.0087 (4)
χ^2	5.00	5.01	4.11
R_p	3.25	4.76	5.64
R_{wp}	4.21	6.18	7.40
R_{Bragg}	4.13	4.40	7.84
No. of parameters	38	36	38

in the atomic positions and thermal parameters were calculated in accordance with Berar & Lennan (1991).

3. Results and discussion

The refined parameters and the corresponding reliability factors (R_p profile R value, R_{wp} weighted profile R value) are summarized in Table 2.† The four cell parameters change as expected for an increasing size of the halogen substituents in the halogenoacetate. This is a strong indication that the three compounds are isostructural. The crystallographic parameters of lithium chloroacetate, lithium bromoacetate and lithium iodoacetate are given in Tables 3–7. Figs. 1–3 show the observed and calculated diffractograms of the three compounds with a difference plot.

In addition to the refinements described in the *Experimental*, we have carried out further refinements with independent isotropic thermal displacement factors for all non-halogen atoms on one hand and for rigid molecules with a fixed ideal geometry on the other hand. The changes in the resulting R values provided a good test for the reliability of the obtained structure model. The refinement with unconstrained isotropic thermal displacement factors for non-halogen remained stable, but gave only minor improvements in R_p (3.21 for chloroacetate, 4.74 for bromoacetate and 5.53 for iodoacetate), therefore, the introduction of four additional parameters appeared not necessary. For another test of the structural model, bond lengths and angles within the halogenoacetate anion were fixed to the following 'chemically true' values: Cl—C 1.76, Br—C 1.90, I—C 2.00, C—C 1.54, C—O 1.35 Å, Cl—C—C 109.8 and C—C—O = O—C—O 120°. These restrictions resulted in only slightly worse agreement factors (R_p = 4.65 for chloroacetate, 5.94 for bromoacetate and 6.56 for iodoacetate). This indicates that the diffraction pattern as calculated for the ideal molecular geometry is very similar to the observed pattern. Note that the structure was solved *ab initio* without any assumptions concerning the geometry of the molecule. The determination of bond geometries with high accuracy and of reliable atomic displacement parameters is beyond the capability of the applied method. Consequently, some of the values given in Table 7 appear chemically unreasonable. This is especially the case for lithium iodoacetate where the strong scattering power of iodine dominates the diffractogram. However, we were mainly interested in gaining information about the packing of the molecules in the crystal in order to understand the solid-state reactivity.

The molecular structure of lithium bromoacetate together with atom labeling is shown in Fig. 4. A packing plot of the structure of lithium bromoacetate is shown in Fig. 5. The structure consists of slabs of bromoacetate anions with neighboring Br atoms. The slabs are sepa-

† Supplementary data for this paper are available from the IUCr electronic archives (Reference: HR0041). Services for accessing these data are described at the back of the journal.

rated by layers of lithium ions. Each lithium ion is situated in the center of an oxygen tetrahedron formed by O atoms belonging to four different halogenoacetate anions. Two LiO_4 tetrahedra are linked by common edges and these pairs of tetrahedra are interconnected by sharing edges to build up layers in the *bc* plane with six-membered rings. Fig. 6 gives a view on the *bc* plane (parallel to one slab of LiO_4 tetrahedra), where only O atoms are shown for clarity.

The structure-determining force in these structures is the strong electrostatic interaction between lithium cation and carboxylate. There is also some hydrophobic interaction between the halogen atoms (Desiraju, 1995), but energetically this should be a minor effect. Neighboring layers of molecules are separated along the *a* direction by double-layers of halogen atoms (*X*), as shown in Fig. 7 for a view parallel to [010]. The shortest non-bonding *X*—*X* distances in the *a* direction are 3.899 (Cl), 3.855 (Br) and 3.946 Å (I). In the *b* direction, the shortest *X*—*X* distance is equivalent to the unit-cell length *b*: 4.845 (Cl), 4.861 (Br) and 4.892 Å (I). For chlorine and bromine these values are considerably larger than the sum of *X*—*X* van der Waals radii (Cl—Cl 3.5, Br—Br 3.7 Å), indicating that the two adjacent halogen layers do not form a close packing in this case.

Table 3. *Fractional atomic coordinates and equivalent isotropic displacement parameters (Å^2) for lithium chloroacetate*

$$U_{eq} = (1/3)\Sigma_i\Sigma_j U^{ij} a^i a^j \mathbf{a}_i.\mathbf{a}_j.$$

	x	*y*	*z*	U_{eq}
Cl(1)	0.3600 (7)	0.139 (1)	0.1519 (7)	0.108
O(1)	0.112 (1)	0.316 (2)	0.962 (1)	0.005
O(2)	0.098 (2)	−0.051 (3)	0.826 (1)	0.005
C(1)	0.148 (2)	0.089 (3)	0.933 (2)	0.005
C(2)	0.279 (2)	−0.093 (3)	0.008 (2)	0.005
Li(1)	−0.007 (4)	0.583 (7)	0.856 (4)	0.005

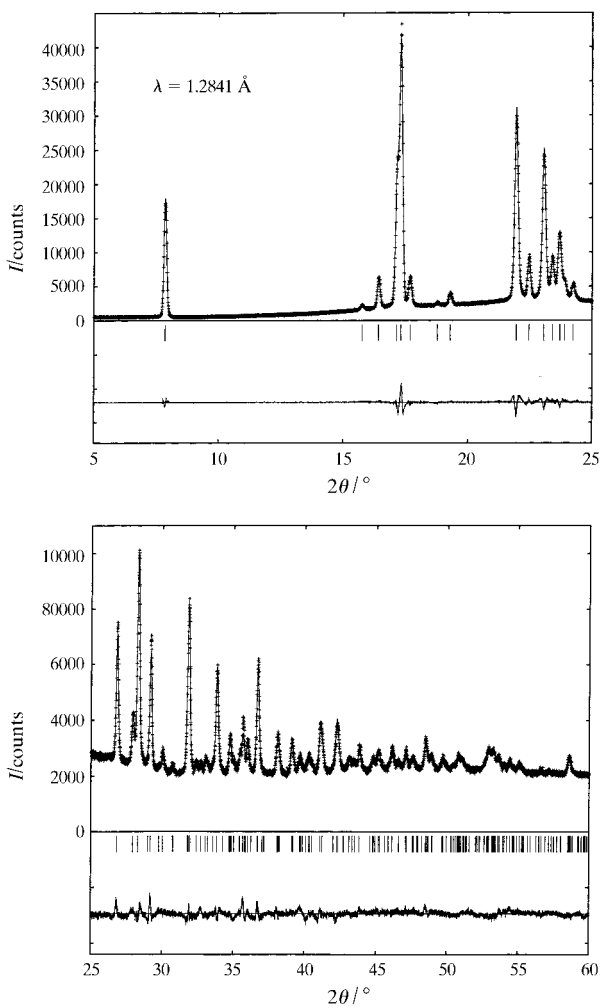

Fig. 1. Observed and calculated patterns together with a difference plot for lithium chloroacetate, split into two regions.

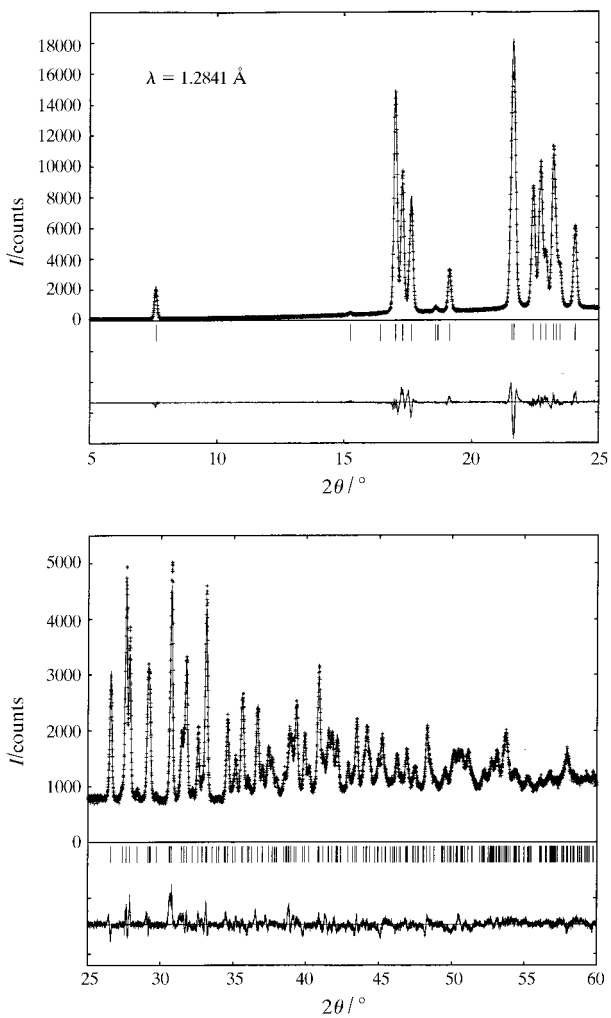

Fig. 2. Observed and calculated patterns together with a difference plot for lithium bromoacetate, split into two regions.

Table 4. *Fractional atomic coordinates and equivalent isotropic displacement parameters (Å^2) for lithium bromoacetate*

$U_{eq} = (1/3)\Sigma_i\Sigma_j U^{ij} a^i a^j \mathbf{a}_i.\mathbf{a}_j.$

	x	y	z	U_{eq}
Br(1)	0.3679 (3)	0.1644 (7)	0.1544 (5)	0.058
O(1)	0.102 (1)	0.305 (4)	0.969 (2)	0.004
O(2)	0.089 (2)	−0.067 (3)	0.824 (2)	0.004
C(1)	0.140 (3)	0.070 (5)	0.921 (3)	0.004
C(2)	0.269 (2)	−0.083 (5)	0.010 (3)	0.004
Li(1)	0.000 (5)	0.60 (1)	0.858 (6)	0.004

Table 5. *Fractional atomic coordinates and equivalent isotropic displacement parameters (Å^2) for lithium iodoacetate*

$U_{eq} = (1/3)\Sigma_i\Sigma_j U^{ij} a^i a^j \mathbf{a}_i.\mathbf{a}_j.$

	x	y	z	U_{eq}
I(1)	0.3739 (4)	0.181 (2)	0.1504 (8)	0.12
O(1)	0.106 (5)	0.32 (1)	0.953 (7)	0.038
O(2)	0.078 (3)	−0.07 (1)	0.831 (6)	0.038
C(1)	0.127 (8)	0.07 (2)	0.94 (1)	0.038
C(2)	0.249 (5)	−0.09 (1)	0.039 (9)	0.038
Li(1)	0.01 (1)	0.51 (4)	0.81 (2)	0.038

In the case of iodine the minimal distance between halogen atoms in the *a* direction is equivalent to the sum of van der Waals radii (I—I 4.0 Å). We ascribe this to the structure-directing effect of the small lithium cation that coordinates to the carboxy groups and thereby restricts the possible arrangements of the halogen atoms (that may pack more densely otherwise). This is underscored by the comparatively high atomic temperature factors for the halogen atoms compared with the non-halogen atoms which points to some degree of packing disorder within the halogen layers. Furthermore, it is interesting to note that the elongation of the *a* axis in the row Cl–Br–I is only partially due to the increasing radius of *X*, but is also caused by reorientation of the molecules themselves.

Silver chloroacetate and sodium chloroacetate readily undergo a solid-state polymerization with elimination of silver chloride and sodium chloride, respectively. Their structures (Epple & Kirschnick, 1997; Elizabé *et al.*, 1997), although completely different from each other with respect to the packing of the molecules, support a topochemical polymerization mechanism. The silver chloroacetate structure is composed of carboxylic acid-like dimers with two silver ions bridging two chloro-

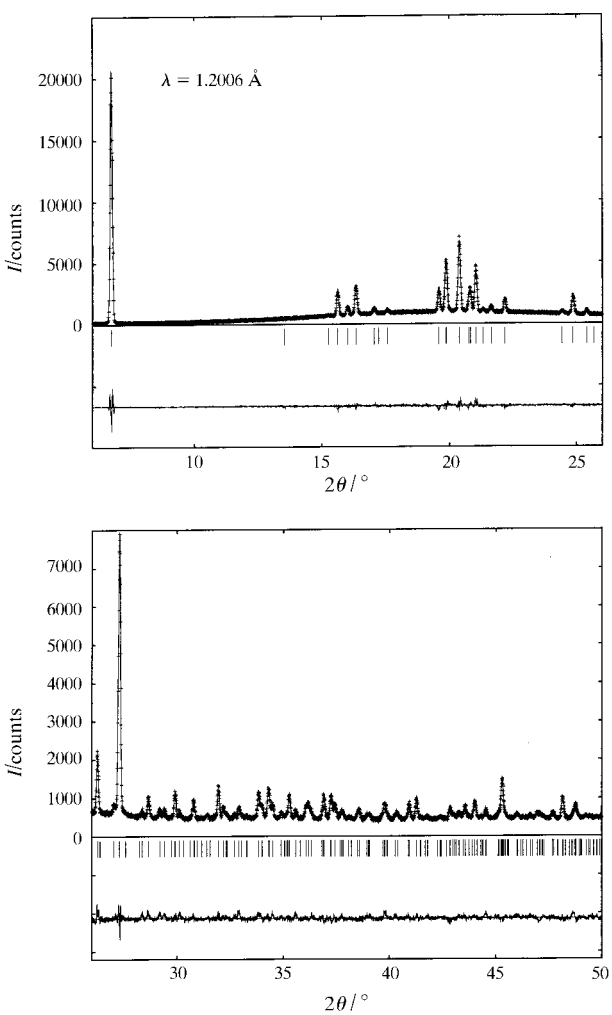

Fig. 3. Observed and calculated patterns together with a difference plot for lithium iodoacetate, split into two regions.

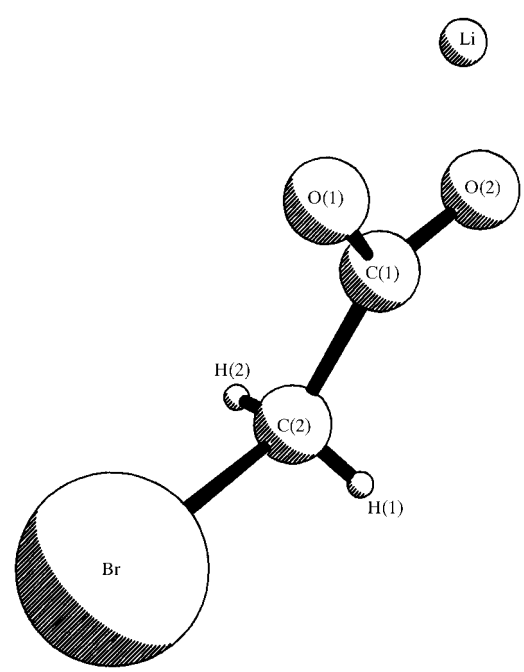

Fig. 4. Molecular structure of lithium bromoacetate with labeling. The other two title compounds have the same structure.

Table 6. *Atomic temperature factors B for halogen (B_{eff}; anisotropic refinement) and for non-halogen atoms (B_{iso}; for C, O, Li; isotropic refinement)*

$$B = 8\pi^2 U.$$

Compound	B_{eff} (Å^2)	B_{iso} (Å^2)
Lithium chloroacetate	8.54	0.4 (2)
Lithium bromoacetate	4.60	0.3 (2)
Lithium iodoacetate	9.49	3.0 (1)

acetate anions. A short Ag—Cl distance is observed between neighboring molecules (2.903 Å compared with 2.775 Å in silver chloride). Together with a suitable stacking of the silver chloroacetate molecules, a possible reaction mechanism can be derived. The situation is less obvious for sodium chloroacetate, where the molecules are oriented in a similar manner as in the lithium salts: the halogen substituents point to each other and the sodium cations form a layer between the carboxy groups, each sodium cation being coordinated by six O atoms. There is no short Na—Cl distance as in silver chloroacetate. Still, a topochemical polymerization can be rationalized in this case along the *b* axis with a nucleophilic attack of carboxy groups on neighboring methylene C atoms.

In contrast to that, the structures of the three lithium salts appear to be less prone to a solid-state reaction as no short distance between lithium and halogen is present (as in silver chloroacetate), and the orientation between neighboring halogenoacetate anions appears to be unfavorable for a polymerization. Another explanation could be the strong polarizing effect of the small lithium cation that prevents the carboxy groups from attacking neighboring molecules at the methylene carbon. This can be visualized by a strong 'fixation' of the carboxylic groups by the lithium cation that dominates the crystal packing.

Energetically, this reaction type is driven by the large lattice energy of the alkali halides that are formed (*e.g.* LiCl, AgCl, NaCl). It would be of high interest to compute the free energy of reaction for the polymerization of $LiOOCCH_2—X$ to Li*X* and polyglycolide. Unfortunately, no enthalpy of formation ΔH (let alone free enthalpy of formation ΔG) is known for any halogenoacetate (the values for *MX* and polyglycolide are reported; Lebedev *et al.*, 1978), therefore, we cannot distinguish at this stage between thermodynamic and kinetic control, the latter being due to an unfavorable packing and restricted mobility of the reactants in the crystal.

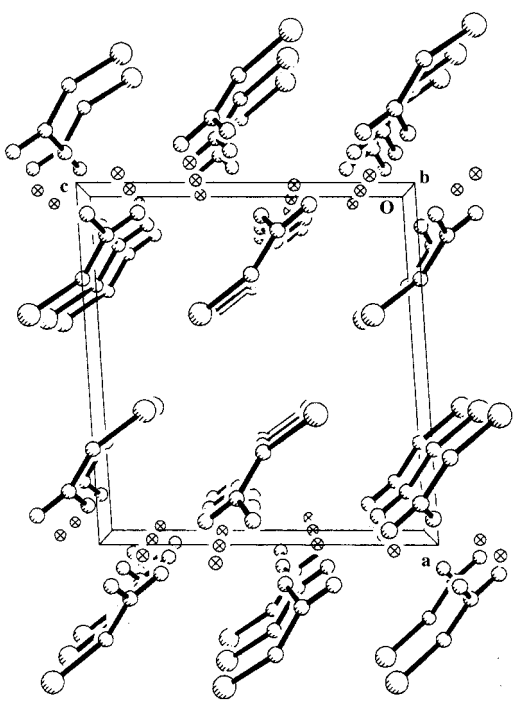

Fig. 5. Packing plot of lithium bromoacetate, viewed on the *ac* plane. The molecules are stacked in slabs with halogen atoms and carboxylate groups pointing to each other, respectively. Layers of lithium ions join neighboring carboxylate groups.

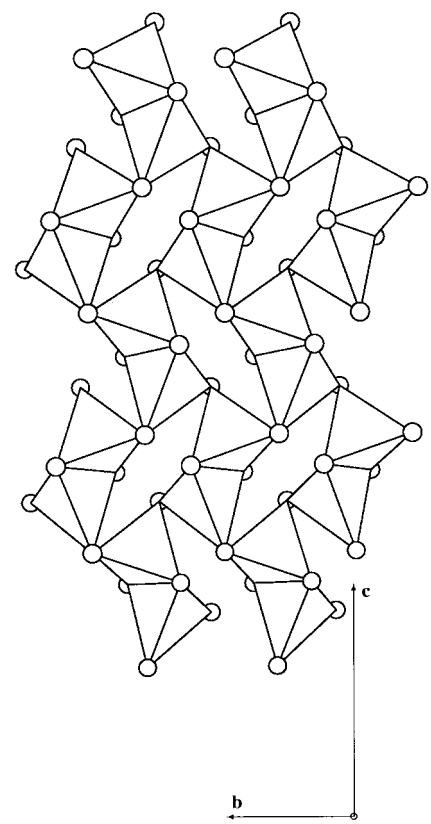

Fig. 6. View on the *bc* plane (parallel to one slab of LiO_4 tetrahedra) in lithium bromoacetate with only O atoms shown. Six-membered rings are formed by corner-linked pairs of edge-linked LiO_4 tetrahedra.

Table 7. *Selected atomic distances (in Å) and angles (in °) of the three lithium halogenoacetates*

Lithium chloroacetate		Lithium bromoacetate		Lithium iodoacetate	
Cl—C2	1.84	Br—C2	1.97	I—C2	2.07
C1—C2^{i}	1.62	C1—C2^{i}	1.62	C1—C2^{i}	1.68
C1—O1	1.19	C1—O1	1.29	C1—O1	1.21
C1—O2	1.24	C1—O2	1.18	C1—O2	1.33
Li—O1	1.91	Li—O1	1.99	Li—O1	1.78
Li—O1^{ii}	2.03	Li—O1^{ii}	1.97	Li—O1^{ii}	2.63
Li—O2^{iii}	1.91	Li—O2^{iii}	1.99	Li—O2^{iii}	1.63
Li—O2^{iv}	2.06	Li—O2^{iv}	1.85	Li—O2^{iv}	2.14
C1^{i}—C2^{i}—C1	102.7	Br^{i}—C2^{i}—C1	111.9	I^{i}—C2^{i}—C1	110.2
O1—C1—O2	125.5	O1—C1—O2	129.7	O1—C1—O2	121.7
C2^{i}—C1—O1	129.6	C2^{i}—C1—O1	117.8	C2^{i}—C1—O1	125.0
C2^{i}—C1—O2	104.7	C2^{i}—C1—O2	112.3	C2^{i}—C1—O2	111.1
O1—Li—O1^{ii}	93.5	O1—Li—O1^{ii}	91.4	O1—Li—O1^{ii}	82.0
O2^{iii}—Li—O2^{iv}	111.7	O2^{iii}—Li—O2^{iv}	114.1	O2^{iii}—Li—O2^{iv}	116.9
O1—Li—O2^{iii}	113.9	O1—Li—O2^{iii}	119.6	O1—Li—O2^{iii}	133.9
O1—Li—O2^{iv}	112.3	O1—Li—O2^{iv}	106.5	O1—Li—O2^{iv}	107.8

Symmetry codes: (i) $x, y, z+1$; (ii) $-x, 1-y, 2-z$; (iii) $-x, \frac{1}{2}+y, \frac{3}{2}-z$; (iv) $x, y+1, z$.

It must be emphasized that the type of solid-state reaction discussed here differs from classical photopolymerization reactions in an important aspect: the reaction leads to a heterogeneous mixture of two components (salt *MX* and polyglycolide), separated on the μm scale (Epple & Herzberg, 1997). Thus, considerable diffusion has to occur. Consequently, a favorable arrangement of molecules in the parent crystal, *i.e.* the halogenoacetate, can only serve as an indication for the reaction course, but can never explain it completely. Note that there are cases of molecular solid-state reactions where it was demonstrated that the reaction occurs at defects in the crystal and where the parent crystal structure even suggested a wrong reaction product (Thomas, 1979).

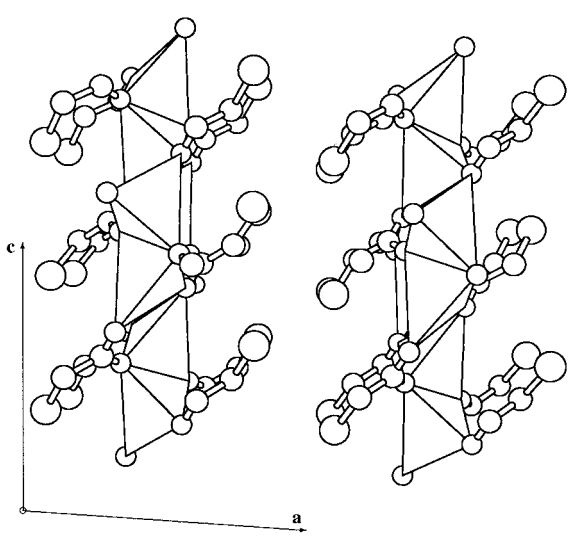

Fig. 7. Two chains of interconnected LiO_4 tetrahedra in the *ac* plane in lithium bromoacetate, together with the remainder of the molecules. Li atoms are located in the centers of edge-sharing LiO_4 tetrahedra that form layers in the *bc* plane. The halogen atoms of two adjacent layers are oriented towards each other (same perspective as in Fig. 5).

The three additional structures of halogenoacetates reported here help to understand the reactivity of this class of compound. Within the row of lithium chloroacetate, sodium chloroacetate and silver chloroacetate, all crystal structures are now known. Although the anion is identical in all cases, the arrangement of the molecules and even the coordination of the cation is completely different. We may therefore conclude that the nature of the cation (polarizing effect and ion size) dominates the structure and thereby the solid-state reactivity. This is in good agreement with the experimental results of the polymerizability of different halogenoacetates (Table 1).

Generous financial support from the Deutsche Forschungsgemeinschaft (Heisenberg grant for ME) and the Fonds der Chemischen Industrie is gratefully acknowledged. We thank Dr S. E. Doyle for experimental assistance. We also want to thank Professor H. Fuess (Darmstadt) and Professor A. Reller (Hamburg) for support during these experiments. We are grateful to HASYLAB for allocation of beamtime. Beamline B2 at HASYLAB is supported by the Bundesminister für Bildung und Forschung (grant No. 05647 RDA8).

References

Berar, J. F. & Lennan, P. (1991). *J. Appl. Cryst.* **24**, 1–5.
Boldyrev, V. V. (1990). *React. Solids*, **8**, 231–246.
Chiellini, E. & Solaro, R. (1996). *Adv. Mater.* **8**, 305–313.
Desiraju, G. R. (1995). *Angew. Chem. Int. Ed. Eng.* **34**, 2311–2327.

Dinnebier, R. E., Behrens, U. & Olbrich, F. (1997*a*). *Organometallics*, **16**, 3855–3858.
Dinnebier, R. E., Pink, M., Sieler, J. & Stephens, P. W. (1997*b*). *Inorg. Chem.* **36**, 3398–3401.
Elizabé, L., Kariuki, B. M., Harris, K. D. M., Tremayne, M., Epple, M. & Thomas, J. M. (1997). *J. Phys. Chem. B*, **101**, 8827–8831.
Enkelmann, V. (1984). *Adv. Polym. Sci.* **63**, 91–136.
Epple, M., Ebbinghaus, S., Reller, A., Gloistein, U. & Cammenga, H. K. (1995). *Thermochim. Acta*, **269/270**, 433–441.
Epple, M. & Herzberg, O. (1997). *J. Mater. Chem.* **7**, 1037–1042.
Epple, M. & Kirschnick, H. (1996). *Chem. Ber.* **129**, 1123–1129.
Epple, M. & Kirschnick, H. (1997). *Chem. Ber.* **130**, 291–294.
Epple, M., Sankar, G. & Thomas, J. M. (1997). *Chem. Mater.* **9**, 3127–3131.
Epple, M., Sazama, U., Reller, A., Hilbrandt, N., Martin, M. & Tröger, L. (1996). *J. Chem. Soc. Chem. Commun.* pp. 1755–1756.
Epple, M. & Seifert, R. (1996). *J. Solid State Chem.* **121**, 129–132.
Epple, M. & Tröger, L. (1996). *J. Chem. Soc. Dalton Trans.* pp. 11–16.
Harris, K. D. M., Johnston, R. L. & Kariuki, B. M. (1998). *Acta Cryst.* A**54**, 632–645.
Kariuki, B. M., Zin, D. M. S., Tremayne, M. & Harris, K. D. M. (1996). *Chem. Mater.* **8**, 565.
Lebedev, B. V., Yevstropov, A. A., Kiparisova, Y. G. & Belov, V. I. (1978). *Polymer Sci. USSR*, **20**, 32–42.
Pepinsky, R., Okaya, Y. & Mitsui, T. (1957). *Acta Cryst.* **10**, 600–601.
Rodriguez-Carvajal, J. (1990). *Abstracts of the Satellite Meeting on Powder Diffraction of the XV Congress of the IUCr*, Toulouse, France, p. 127.
Schmidt, G. M. J. (1971). *Pure Appl. Chem.* **27**, 647–678.
Sheldrick, G. M. (1985). *SHELXS86. Program for the Solution of Crystal Structures*. University of Göttingen, Germany.
Thomas, J. M. (1974). *Philos. Trans. R. Soc. Ser. A*, **277**, 251.
Thomas, J. M. (1979). *Pure Appl. Chem.* **51**, 1065–1082.
Tremayne, M., Kariuki, B. M. & Harris, K. D. M. (1996). *J. Appl. Cryst.* **29**, 211.
Vedavathi, B. M. & Vuayan, K. (1977). *Acta Cryst.* B**33**, 946–948.
Wegner, G. (1977). *Pure Appl. Chem.* **49**, 443–454.
Wei, K. T. & Ward, D. L. (1976). *Acta Cryst.* B**32**, 2768.
Werner, P. E., Eriksson, L. & Westdahl, M. (1985). *J. Appl. Cryst.* **18**, 367–370.